RASĀYAN *J. Chem.*
Vol. 19 | No. 3 | 1322-1330 | July-September | 2026
ISSN: 0974-1496 | e-ISSN: 0976-0083 | CODEN: RJCABP
http://www.rasayanjournal.com
http://www.rasayanjournal.co.in

EQUILIBRIUM STUDY OF THERMODYNAMIC AND KINETIC OF ACTIVATED CARBON ENSUING FROM *Azadirachta indica* BARK L ACTIVATED CARBON ACIDIC DISPERSION FOR THE REMOVAL OF METHYLENE BLUE DYE

A. Sivakumar✉, N. Punitha, and M. Mangalam
PG and Research Department of Chemistry, Rajah Serfoji Government College (Autonomous), Thanjavur-613005, (Affiliated to Bharathidasan University, Tiruchirapalli, Tamil Nadu, India
✉Corresponding author: mietsivakumar@gmail.com

ABSTRACT
The investigations on the removal of Methylene Blue dye from aqueous solutions by adsorbent utilising *Azadirachta indica* Bark L Activated Carbon charcoal were conducted under a broad range of experimental designs and optimisation settings. The adsorption equilibrium approach has been used to investigate each of the factors. The Langmuir, Freundlich, and Tempkin adsorption isotherms were employed to assess the adsorption isotherm. Calculations were made for thermodynamic parameters such Δas H^o, ΔS^o and ΔG^o. It illustrated how the adsorption was endothermic and spontaneous. The fake second-order kinetics made much more sense than the pseudo-first-order kinetic model. FT-IR, SEM, AFM, BET, and powder XRD were used to measure it both before and after the adsorption of a substance that resembled the colour Congo red in water.
Keywords: Adsorption, Isotherm, Powder XRD, Activated Charcoal, BET, AFM, and Methylene Blue Dye.
RASĀYAN*J. Chem.*, Vol. 19, No. 3, 2026

INTRODUCTION

Wastewater generated from the food, beverage, paint, textile, wool, carpet, tannery, printing, electroplating, paper, and pulp industries, among others, contains colours, surfactants, heavy metals, and salts, among other things.[1,2] In the textile processing industry, colour is often added using pigments and colourants. When colouring, excess water escapes as effluents, and because of their toxicity, they are considered pollutants. Inhalation, swallowing, skin sensitivity, eye irritation, cancer, and respiratory problems are all brought on by this dust-carcinogenic substance.[2,3] It is so challenging to forecast the behaviour of hazardous dyes in effluents to stop pollution of the environment at its source. To assess the toxicity of the effluent, one can use fundamental dyeing features such as cloth weight, shade depth, and colour production from dye sulphur, such as fixing. The industry can cut waste because the predictions reflect positive outcomes.[4] these techniques consist of chemical oxidation, photo-oxidation, ozonation, coagulation, and photo-catalysis. Adsorption onto inorganic or organic matrices, followed by microbial degradation.[5]

In the nation, removing dyestuff from municipal wastewater or effluents can be accomplished with great success using adsorption[6,7] Partheniumhysterophorus[8] rice flour[9] pine sawdust[10] wood sawdust and rubber[11] de-oiled soya and bottom-up ash[12] a palm kernel[13] crow feathers[14] and so on. The previously mentioned literature study led to the decision to employ *Azadirachta indica* Bark L Activated Carbon (AIBAC), a cheap and readily available adsorbent material that effectively adsorbs the most famous natural blue dye source (indigo). Widely used for centuries in textiles.

EXPERIMENTAL

Materials

Carbon activated from *Azadirachta indica* Bark L was employed as an adsorbent to bind the aqueous solution of Congo red dye. Each and every reagent (E-Merck and SD-fine, India) needed for this experiment is readily accessible. Analar level.

The Process of Making Activated Carbon

The *Azadirachta indica* Bark L.-based activated carbon was sourced locally for essential components. After being cut into tiny pieces and dried, the material was rinsed with hot distilled water to get rid of any last bits of dirt. It was then impregnated with a strong sulfuric acid solution. A weight-to-acid volume ratio of 0.5:1 is applied to the material during impregnation. It was rinsed on a regular basis after the roasted material was cleaned with simple water until the pH reached a neutral level. The material was carbonised in a muffle furnace following 500 °C drying. In the end, activated carbon was produced by grinding and sieving it.

Adsorption Studies

The dye solution consisted of 1000 mg/L of dye dissolved in the prescribed amount of water. This solution was used as the stock solution for all of the experimental investigations, using two different distilled waters and Methylene Blue colourant. For every investigation, double-distilled water was utilised. The training set methodology was employed in the adsorption testing. The iodine flask was once more filled with 100 mg of adsorbent and 100 ml of MBD at a predetermined concentration. Subsequently, the blend was repeatedly homogenised in a water bath that was temperature-controlled (Techno). Methylene Blue colourant concentration was measured using a spectrophotometer calibrated at 668 nm. The filtrate was consistently present, and the solutions were shook periodically. The examination is done once more.

$$\text{Adsorption capacity } q_e = \frac{(C_o - C_e)}{W} \text{ V} \quad (1)$$

Where V represents the volume (mL) in the MBD solution, W is the weight (g) of the AIBAC (g), C_o is the starting point (mg/L) amount in the MBD solution, and C_e represents the final (mg/L) solution concentrations.

RESULTS AND DISCUSSION

The Effects of Adsorbent Quantity, pH, Time, and Contact

In the previously stated research, adsorbents with sizes ranging from 50 to 300 mg were employed. A 10 mg/L solution of Methylene Blue dye was added to 100 ml of a shaken well mixture in randomly selected volumes. Based on the results, it was found that a dosage of 100 mg, an agitation period of 100 min, and a pH of 10.0 were the perfect values to extract the maximum quantity of MBD solution.[15]

Separation of the Initial Concentration and Temperature

The time at equilibrium was determined independently of the initial MBD (C_o) concentration. The results are shown in Table-1 and indicate that an increase in the driving force of mass transfer causes an increase in the amount of MBD adsorbed (q_e) when the starting concentration of MBD rises. Dissolving the initial concentration in an aqueous solution can successfully overcome mass transfer resistances in a solid medium.[16] Between 30 and 50 °C saw an increase in the proportion of MBD removal. The adsorption process's endothermic characteristic has been shown.

Table-1: Optimal Conditions and the Removal of MBD from AIBAC

Primary conc. of MBD (C_o)mg/L	Equilibrium Conc. of MBD (C_e), mg/L			Amount of MBD adsorbed at equilibrium (q_e), mg/g			MBD Removal (%) by AIBAC		
	30°C	40°C	50°C	30°C	40°C	50°C	30°C	40°C	50°C
10	2.227	1.318	0.864	7.773	8.682	9.316	77.73	86.82	91.36
20	7.182	5.818	5.364	12.818	14.182	14.636	64.09	70.91	73.18
30	14.409	13.591	12.227	15.591	16.409	17.773	51.97	54.70	59.24
40	22.227	20.182	17.682	17.773	19.818	22.318	44.43	49.55	55.80
50	29.818	27.591	24.864	20.182	22.409	25.136	40.36	44.82	50.27

Adsorption Isotherms

The colourant is applied and examined using the Tempkin, Freundlich, and Langmuir isotherm systems. A 2017 study found the optimal link between the adsorption capacity (q_e) in the rock-solid and fluid

phases and the adsorbate concentrations (C_e) in the bulk fluid phase.[17] the linear version of the rearranged Langmuir model is shown below with reference to.[18]

$$\frac{C_e}{q_e} = \frac{1}{Q_0 b_L} + \frac{C_e}{Q_0} \quad (2)$$

Based on the plot's slope and intercept (C_e) / (q_e), the constants Q_0 and b_L can be computed. The Freundlich equation's linear version is shown in the following.[18]

$$\log q_e = \log k_f + \frac{1}{n} \log C_e \quad (3)$$

The Langmuir constants Q_o and b_L are related to the monolayer adsorption energy (L/mg) and capability (mg/g) of the Freundlich isotherm, whereas the empirical constants of the isotherm have been attempted to be changed. The measurements indicate the adsorption force and capacity (mg^{-1} 1/n L 1/m g^{-1}) in accordance. The sort of final MBD concentration in solution is denoted by the abbreviation Ce. Figure-2 depicts the Freundlich adsorption isotherm, $\log q_e$ vs. $\log C_e$, while Fig.-1 illustrates the Langmuir adsorption isotherm for MBD adsorption on AIBAC, C_e/qe Vs. C_e. Lower temperatures may be preferable for adsorption, according to the monolayer adsorption capacity measurements (Q_o), which increase with temperature. Because colours diffuse into AIBAC more quickly at lower temperatures, this finding makes sense. The adsorption energy indicates that. According to this study, high temperatures promote adsorption. At increasing temperature, there are actually only minor variations in the adsorption intensity (n) values. The heat of adsorption is thought to be linear, as opposed to logarithmic, based on the Tempkin isotherm. This is a description of the linear Tempkin Isotherm model.[19]

$$q_e = \frac{RT}{b_r} \ln a_T + \frac{RT}{b_r} \ln \quad (4)$$

The universal gas constant (J K^{-1} mol^{-1}) is denoted by R, while the adsorption heat is represented by b_T. Temperature (K), symmetry binding constant (L/mg) (a_T), and (kJ mol^{-1}) are all given by T. Together with qe and $\ln C_e$, the Tempkin isotherm is displayed in Fig.-3. The MBD adsorption has been given to the binding free energy and adsorption heat, and the Tempkin constants a_T and b_T during binding constant values at equilibrium are obtained using the heat of adsorption, the intercepts, and the slope of the C_e plot. Table-2 displays the adsorption equilibrium data.

Table-2: Adsorption of MBD on AIBAC: The Outcomes from the Isotherm Model

Temp.	Langmuir Isotherm			Freundlich Isotherm			Tempkin Isotherm		
	r^2	Q_0 (mg/g)	b_L (L/mg)	r^2	k_f	n	r^2	b_T ($kJmol^{-1}$)	a_T (L/mg)
30	0.994	23.009	0.181	0.996	5.991	2.789	0.994	10.586	3.852
40	0.996	24.331	0.249	0.993	8.032	3.333	0.997	9.774	6.988
50	0.979	27.473	0.257	0.989	9.253	3.339	0.958	10.382	8.672

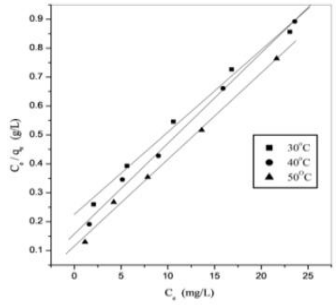

Fig.-1: Langmuir isotherm for the Adsorption of MBD on AIBAC

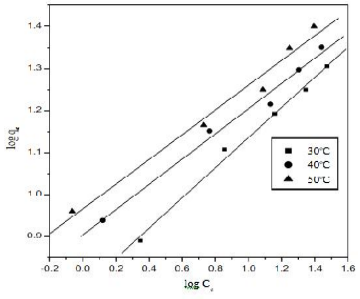

Fig.-2: Freundlich isotherm for the Adsorption of MBD on AIBAC

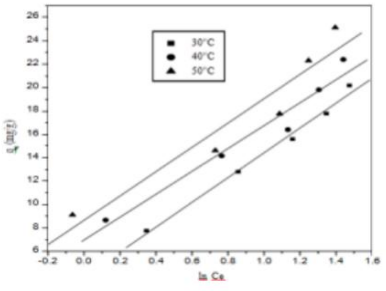

Fig.-3: Tempkin isotherm for the adsorption of MBD on AIBAC

Thermodynamic Aspects

The modifications in entropy (G^o), free energy (G^o), and enthalpy (H^o) have all been determined by utilising the thermodynamic equilibrium constant (K_o) and (S^o). According to the article's method[20] consistent values show the adsorption mechanism's equilibrium. Equations one and two above alter the fundamental concepts of thermodynamics.

$$LnK_o = \frac{\Delta S^0}{R} - \frac{\Delta H^0}{RT} \quad (5)$$

$$\Delta G^o = -RTlnK_o \quad (6)$$

The standard entropy change (J $K^{-1}mol^{-1}$) is represented by ΔS^o, the maximum change in infinite energy (k J mol^{-1}) is represented by ΔG^o, and the normal adsorption enthalpy is H^o (k J mol^{-1}). The values ΔH^o and ΔS^o are obtained by plotting lnK_oVs 1/T and examining the graph's slope and intercept. Table-3 displays the enthalpy, standard free energy, and equilibrium constants. These findings imply that a spike in temperature led to an endothermic adsorption, which in turn produced a jump in K_o. It is evident that the initial concentration of MBD increases with the standard free energy values. In support of the observation of spontaneous adsorption, standard free energy values were found to be negative. Enthalpy change values between 15 and 45 have been noted. These data demonstrated the endothermic nature of the physical contacts and adsorption process between the AIBAC and the MBD. The traditional entropy values for the adsorption of MBD on AIBAC were positive and varied from 50 to 159 $JK^{-1}mol^{-1}$. It was found that the MBD adsorption on AIBAC significantly impacted the solid-solution interface.[21]

Table-3: Thermodynamic Parameters for the Adsorption of MBD on AIBAC

C_o (mg/L)	K_o			ΔG^o(kJ mol^{-1})			ΔH^o (kJ mol^{-1})	ΔS^o (JK^{-1} mol^{-1})
	30°C	40°C	50°C	30°C	40°C	50°C		
10	3.490	6.586	10.579	-3.148	-4.905	-6.335	45.170	159.659
20	1.785	2.437	2.729	-1.459	-2.319	-2.696	17.351	64.997
30	1.082	1.207	1.454	-0.199	-0.490	-1.004	11.972	62.341
40	0.800	0.982	1.262	-0.563	-0.047	-0.625	18.549	59.281
50	0.677	0.812	1.011	-0.983	-0.547	-0.029	15.963	50.488

Adsorption Equilibrium Investigate

A variety of kinetic models, such as the models of misleading first and second categories developed by Lagergren, are used to examine the data gathered from batch studies. Representing the characteristics of the integrated pseudo-first order kinetic form, the amounts of MBD adsorbed on AIBAC at equilibrium and time t, respectively, are represented by q_e and q_t, while the pseudo-first order rate constant (min^{-1}) is shown by k_1. Since the adsorption is dominated by first-order kinetics, a regular approach between the two parameters, log (q_e-q_t) and t, is thus expected. With the values of k_1 and qe, it is possible to evaluate the slope and intercept of the first-order plot. If first-order kinetics is unable to sufficiently explain the adsorption, a pseudo-second order kinetic model may be employed.

$$\log (q\_e-q\_1) = \log q\_e-k\_1/2.303\ t \quad (7)$$

The Representation of the Linear System for the Pseudo-Second Order Model is-

$$t/q_t = [(1/k_2q_e^2) + (1/q_e)t] \quad (8)$$

K_2, or g mg^{-1} min^{-1}, is the fictional second-order rate. A second-order plot's slope and intercept can be used to determine q_e and k_2, and a t / qt graph and t should exhibit a linear connection if the adsorption follows second order. The kinetic data are shown in the first, and parameters of the second order in kinetics are thoughtfully shown in Tables-4 and 5. Between the calculated and experimental results, the pseudo-first order rate equation of adsorption capacity and the bogus second order paradigm agreed well. A strong correlation coefficient ($r^2 = 0.999$) and modest relative variance in percentage terms characterise the experimental results for the adsorption of MBD in a pseudo-second order model. Based on the aforementioned results, a pseudo-second order model that matched a pseudo-first order model was used to obtain the correlation for dye adsorption.[22,23]

Table-4 and 5: Pseudo-first and Second Orders used to Account for the Absorption of MBD on AIBAC

C_o (mg/L)	q_e (exp) (mg/g)	Kinetic model							
		pseudo-first order				pseudo-second order			
		q_e (cal)(mg/g)	k_1 (min^{-1})	r^2	P	q_e (cal)(mg/g)	k_2 (g $mg^{-1}min^{-1}$)	r^2	P
10	7.727	6.904	0.035	0.926	10.65	9.585	0.004	0.976	19.41
20	12.818	7.707	0.013	0.947	39.87	15.291	0.002	0.919	16.17
30	15.591	10.479	0.036	0.876	32.79	17.513	0.004	0.991	10.98
40	17.773	8.076	0.037	0.993	54.56	19.121	0.007	0.999	7.05
50	20.182	8.013	0.015	0.928	60.29	21.786	0.004	0.982	7.37

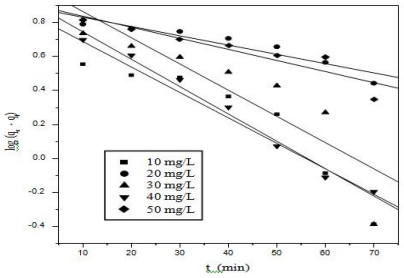

Fig.-4: Pseudo-first order kinetics for the adsorption of MBD on AIBAC

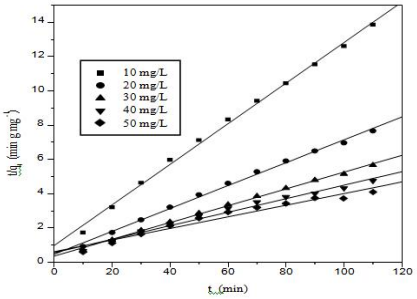

Fig.-5: Pseudo-second-order kinetics for the adsorption of MBD on AIBAC

Infrared Spectroscopic Fourier Transform Studies

The surface's functional groups and related chemical reactivity control the nano-sorbent's porosity and absorbable quantity. Molecules are attracted together when a related entity force is applied because of the imbalance between surface forces and internal pressure caused by this reactivity. Figure-6 displays the FT-IR spectra of AIBAC obtained before adsorption, which are used to assess the type and pattern of adsorption. There was a –OH group present, according to the AIBAC spectrum at 3783 $cm^{-1.}$ A peak at 3409 cm^{-1} and 2922cm^{-1} revealed the presence of the –CH of the alkane stretching group, while the N–H stretching of amines was detected at 3409cm^{-1}. The region at 1591 cm^{-1} showed the N-H bending of the carbonyl stretching group, and at 1704 cm^{-1} the C=O stretching group. The region at 1364cm^{-1} indicated the alkane group –CH stretching. The C-N stretching of aliphatic amines is demonstrated by the areas at 1229cm^{-1}, 1160cm^{-1}, and 1116cm^{-1}. Indicated C-N Stretching of aliphatic amines. Therefore, the Presence of these active groups shows that the participation in the adsorption of dyes on AIBAC.

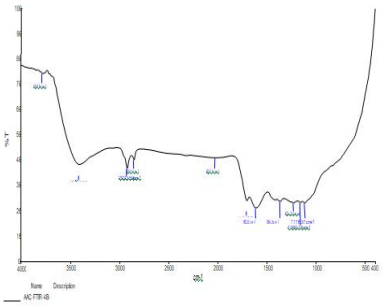

Fig.-6: FT-IR Spectrum before for Adsorption of MBD on AIBAC

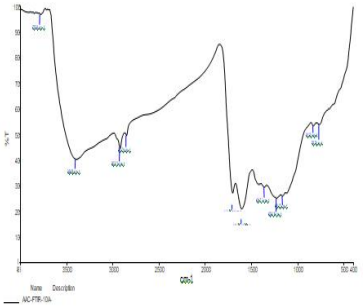

Fig.-7: FT-IR Spectrumafter MBD has been adsorbed on AIBAC, Observed

Studies that used the Scanning Electron Microscope (SEM)

Figures-8 and 9 display scanning electron microscopy pictures of the Methylene Blue dye adsorption process on AIBAC before and after. This clearly showed that before adsorption, AIBAC had a porous structure. There are cave-like pores and openings on its adsorbent surface, which may increase the surface

area that is favourable for adsorption. SEM photos obtained after MBD adsorption clearly demonstrate that MBD has attached itself to the surfaces, pores, and caverns of AIBAC. The structure of AIBAC is changed with the adsorption of MBD, as has been abundantly shown.[20, 21]

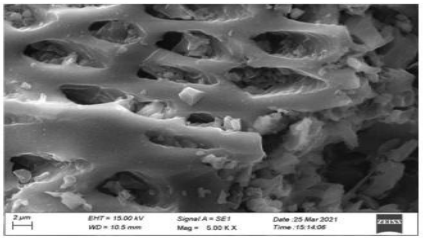

Fig.-8: SEM photograph before the adsorption of MBD on AIBAC

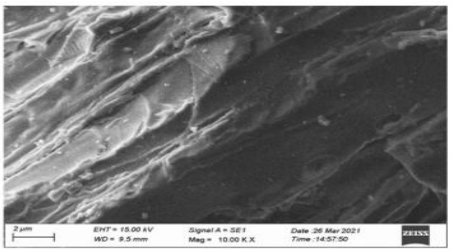

Fig.-9: SEM photograph after adsorption of MBD on AIBAC

Instrumental Analysis

Brunauer Emmett Teller (BET) Analysis

BET theory is used to measure the surface area of solid or porous materials. Generally, it gives evidence on their physical structure, as the area of a material's surface affects how that solid material will interact with its environment. Bark L Activated Carbon (AIBAC) was subjected to BET analysis. The results are mentioned in Table-6 and Fig.-10 is given below.

Table-6: BET Analysis

S. No.	Sample	Surface Area(m^2/g)	Pore Volume(cc/g)	Pore Diameter(nm)
1	AIBAC	27.789	0.031	2.190

The N_2 adsorption-desorption isotherm clearly showed a type - IV isotherms forboth the activated carbon samples, which indicates the presence of the typical meso-porous nature of the carbon Materials as depicted in Fig.-10

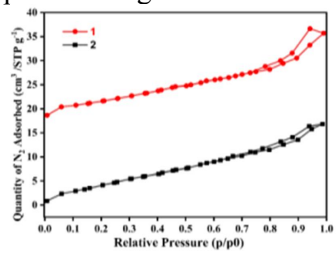

Fig.-10: BET Analysis

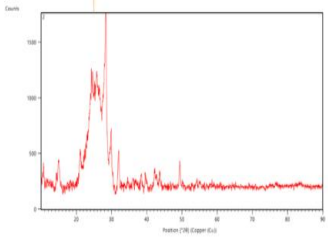

Fig.-11: Powder-XRD Pattern before the Adsorption of AIBAC

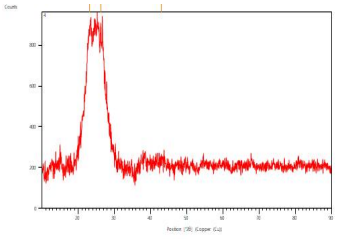

Fig.-12: Powder- XRD Pattern after a Desorption of MBD onto VUSSAC

Powder X–ray Diffraction (P-XRD) Study

The P - XRD (XPERT-3) studies of all the activated carbons before and after adsorption have been conducted. It also provides useful information about structure, shape, size, and crystallinity. The Powder XRD studies are given below.[22]

Table-7: Powder XRD Pattern before Adsorption of AIBAC

Pos. [°2θ]	Height [cts]	FWHM Left [°2θ]	d-spacing [Å]	Rel. Int. [%]
25.5629	1785.00	7.8336	3.48185	100.00

The P-XRD results are tabulated and Fig.-11 Based on the results, the following observations are obtained. The P-XRD data showed that the peak at 25.5629 confirmed the activated carbon peak, and the distorted peaks were observed, showing an amorphous nature of the adsorbent. Therefore, it concludes that the peak position of AIBAC is defined by the temperature at 500 °C. The small intensity peaks were showing the some active functional groups are present in the AIBAC, which are responsible for adsorption. The P-XRD results are tabulated and Fig.-12. Based on the results, the following observations are obtained. The

P-XRD data showed that the peak at 23.1162 confirmed the activated carbon peak, and 26.2752 and 42.9347 confirmed the absorption of MBD and also distorted peaks were observed, which showed has an amorphous nature of the adsorbent. The small intensity peaks were not much shown, which indicated the adsorption of MBD onto AIBAC.

Table-8: Powder XRD Pattern after Adsorption of MBD on AIBAC

Pos.[°2θ]	Height[cts]	FWHMLeft[°2θ]	d-spacing[Å]	Rel. Int. [%]
23.1162	1672.93	2.6765	3.84773	100.00
26.2752	1651.12	2.6765	3.39186	98.70
42.9347	143.11	5.3530	2.10655	8.55

Atomic Force Microscopic (AFM) Study

AFM studies were done before and after the adsorption of dyes onto activated carbons. The AFM technique enables the imaging of almost any type of surface of the materials. The AFM topographical Fig.-13 and Fig.-14 is given below. The surface area (Sa) of the activated carbon VUSSAC before adsorption is 10.273 nm.[23,24]

Table-9: Powder XRD Pattern after Adsorption of MBD on AIBAC

S. No.	Topography	Sa (nm)
1.	AIBAC	52.216
2.	AIBAC+MBD	20.185

The tabulated Sa values concluded that, after adsorption of MBD onto AIBAC were considerably reduced. This is evident from the AFM topographical From AFM studies, it is concluded that the surface of the activated carbons is covered by the dye molecules.

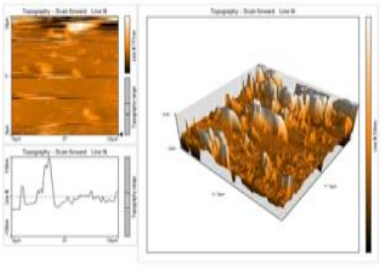

Fig.-13: AFM Study of before Adsorption of AIBAC

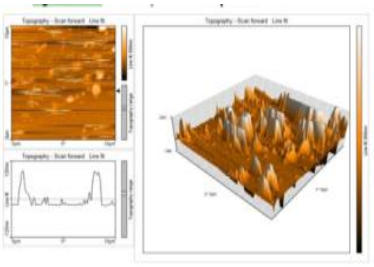

Fig.-14: AFM Study of the after Adsorption of MBD onto AIBAC

CONCLUSION

Azadirachta indica L Bark Activated Carbon (AIBAC) is one readily available, cheap to run and environmentally benign material that can be employed exclusively as an adsorbent to remove MBD from aqueous solutions. The solution's ideal pH is 10.0, its ideal contact time is 120 minutes, and its recommended adsorbent dosage is 100 mg in order to remove MBD. The adsorption capabilities of AIBAC-MBD were illustrated by the adsorption isotherm models that were supplied. FT-IR and SEM data are used to explain the MBD adsorption process. Compared to the pseudo-first order kinetic model, the pseudo-second order kinetic system shows better agreement. The amount of MBD that was eliminated increased from 30 to 50°C.

ACKNOWLEDGMENTS

The Rajah Serfoji Government College, (A) Thanjavur - 613005, Affiliated with Bharathidasan University, Trichirappalli in Tamilnadu, provided the required resources for the writers to complete this study, and they are grateful to them for their assistance.

CONFLICT OF INTERESTS

The authors declare that there is no conflict of interest.

AUTHOR CONTRIBUTIONS

The present work is related to *SDG-6: Clean Water and Sanitation*. All the authors contributed significantly to this manuscript, participated in reviewing/editing and approved the final draft for publication. The research profile of the authors can be verified from their ORCID ids, given below:

A.Sivakumar https://orcid.org/0009-0004-8463-2765
N.Punitha https://orcid.org/0000-0002-2456-5044
M.Mangalam https://orcid.org/0009-0004-2659-887X

Cite this article as: A. Sivakumar *et al.*, *Rasayan J. Chem.*, 19(3), 1322-1330(2026), https://doi.org/10.31788/RJC.2026.1939636

REFERENCES

1. S. P. Raghuvanshi, R. Singh, C.P. Kaushik and A.K. Raghav, *International Journal of Environmental Studies*, **62**, 329(2005), https://doi.org/10.15666/aeer/03035043
2. J. Allen, G. McKay and J.F. Porter, *Journal of Colloid Interface Sciences*, **280**, 322(2004), https://doi.org/10.1016/j.jcis.2004.08.078
3. G.E. Walsh, L.H. Bahnes, W.B. Horning, *Environmental Pollutions*, **A21,** 169(1980), https://doi.org/10.5923/j.textile.20160506.02
4. A. Sivakumar, G. Ramachandranand, P. Thamilarasu, *Annals of Romanian Society for Cell Biology*, **26**, 1915(2021),https://doi.org/10.annalsofrscb.ro/index.php/journal/article/view/11168
5. H. Lata, V.K. Gargand, R.K. Gupta, *An Agricultural Waste*, **74(3)**, 753(2007), https://doi.org/10.1016/j.dyepig.2006.04.007
6. S. D. Khattri, and M.K. Singh, *Adsorption of Science Technonology*, **17(4)**, 269(1999), https://doi.org/10.1177/026361749901700404
7. M. Ozacar and A.I. Sengil, *Bioresource Technology*, **96**, 791(2005), https://doi.org/10.1016/j.biortech.2004.07.011
8. A. Jumasiah, T.G. Chuah, J. Gimbon, T.S.Y. Choong and I. Azni, *Desalination*, **186**, 57(2005), https://doi.org/10.1016/j.biortech.2013.03.048
9. A. Mittal, *Journal of Hazards Mater*, **133**,196(2006), https://doi.org/ 10.1016/j.jhazmat.2005.10.017
10. Olugbenga Solomon Bello and Mohd Azmier, *Environmental Chemistry*, **33(7),** 1298(2007), https://doi.org/ 10.1080/02772248.2011.590490
11. K.Y. Foo and B.H. Hameed, *Chemical Engineering Journal*, **170**, 338(2011), https:// doi.org/10.1016/j.cej.2011.02.068
12. A. SivaKumar, G. RamaChandran and P. Thamilarasu, *Malaysian Journal of Chemistry*, **25(4)**, 38 (2023), https:// doi.org/10.55373/mjchem.v25i4.38
13. I. Langmuir, *Journal of American Chemical Society*, **38(2)**, 2221(1916), https://doi.org/10.1021/acs.jced6b00845
14. R.E,Treybal amd McGraw-Hill, New York, NY, USA, **3**rd edition, (1981), https://doi.org/10.1021/ja02268a002
15. S.Y. Elovich, and O.G. Larinov, Izvestiya Akadmii Nauk SSSR, *Seriya Khimicheskaya*, **2**, 209(1962), https://doi.org/ 10. 4236/ajac.2013.49065
16. B. Stephen Inbaraj and N. Sulochana, *Indian Journal of Chemistry Technology*, **9**, 201(2002), https://doi.org/ 10.1007/s13201- 016-0512-2
17. A. Mashael, A. Ghadahi, and A. Rasmiah, *Journal of Chemistry*, 2013, Article ID 210239(2013), https://doi.org/10.1155/2013/210239
18. Y. S. Ho and G. McKay, *Chemical Engineering Journal*, **70(2)**, 115(1998), https://doi.org/10.1016/S0923-0467(98)00076-1
19. S. Viboon, P. Chiravoot, DuangdaoAht-ong and D. Atong, *Journal of the American Chemical Society*, **22(1)**, 31(2008), https://doi.org/10.1021/ef700285u

20. N. Punitha, R. GanapathiSundaram, G. Vengatesh, R. Rengasamy and J. Elangovan, *Inorganic Chemistry Communication*, **153,** 110732(2023), https://doi.org/10.1016/j.inoche.2023.110732
21. N. Punitha, R. GanapathiSundaram, K. Vijayalakshmi, R. Rengasamy and J. Elangovan, *Journal of Indian Chemical Society*, **99**, 100667(2022), https://doi.org/10.101/j.jics.2022.100667
22. N. Punitha, R. GanapathiSundaram, R. Rengasamy and J. Elangovan, *Chemical Data Collection*, **41,** 100936(2022), https://doi.org/10.10106/j.cdc.2022.100936
23. A.Sivakumar, N.Punitha, M. Mangalam and C.Ganesamoorthi, *Asian Journal of Chemistry* **38(1),** 82(2026), https://doi.org/10.14233/ajchem.2026.34832
24. N.Punitha, A.Sivakumar, A.Parvathipriya, M. Anitha and A.Thamizhanban, *Asian Journal of Chemistry,* **38(3),** 561(2026), https://doi.org/10.14233/ajchem.2026.35352

[RJC-9636/2026]